Pergamon

Int. J. Heat Mass Transfer. Vol. 40, No. 4, pp. 869–879, 1997

0017–9310/97 $17.00 + 0.00

PII: S0017-9310(96)00164-0

Axial void fraction profile in low pressure subcooled flow boiling

O. ZEITOUN

Department of Mechanical Engineering, Faculty of Engineering, Alexandria University, Alexandria, Egypt

and

M. SHOUKRI†

Department of Mechanical Engineering, McMaster University, Hamilton, Ontario L8S 4L7, Canada

(*Received* 12 *September* 1995 *and in final form* 23 *April* 1996)

Abstract—Axial void fraction profiles in subcooled flow boiling in a vertical annulus were obtained using gamma attenuation techniques for different levels of mass flux, wall heat flux and inlet subcooling. A mechanistic model was developed to predict the axial void fraction profile. Various closure relationships were used and a new model, for dividing the wall heat flux between vapour generation and heating the subcooled liquid, was incorporated. The predictions of the proposed model were found to be in good agreement with the present experimental data, as well as other available data, on axial void fraction distribution in low pressure subcooled flow boiling. The proposed mechanistic model does not require prior identification of the location of the onset of significant voids. Copyright © 1996 Elsevier Science Ltd.

1. INTRODUCTION

Subcooled flow boiling is encountered in many industrial applications in the power and process industry. Most of the published work was driven by the needs of the nuclear industry. In nuclear reactors, under certain conditions, subcooled flow boiling may be encountered in the core. Under such conditions, accurate knowledge of the void fraction distribution is required to properly predict the flow stability pressure drop as well as the neutron moderation characteristics. Most available studies focused on high pressure subcooled flow boiling because of its relevance to power reactors. The present work, however, is driven by the need for analysis of low pressure research reactors designed by Atomic Energy of Canada Ltd.

When a subcooled liquid enters a heated channel, the temperature distribution adjacent to the hot surface may result in local boiling at the surface while the bulk of the flow is still subcooled. Bubbles nucleate on the heating surface and may condense as they leave the heating surface and move into the subcooled bulk. The net amount of vapour generation is determined by the difference between the vapour generation rate at the heating surface and the condensation rate in the bulk. Subcooled boiling starts after the heating wall temperature exceeds the saturation temperature enough to cause nucleation at a point called the onset of nucleate boiling (ONB). The subcooled boiling continues downstream from the ONB point but the void fraction cannot grow significantly because of the high subcooling. This low void fraction region continues until the void fraction starts to increase sharply at a location called the net vapour generation (NVG), or the onset of significant void (OSV), point, as depicted in Fig. 1. The NVG point divides the subcooled boiling region, as introduced by Griffith *et al.* [1], into two regions: low void fraction region followed by a second region, in which the void fraction increases significantly. The NVG point is the transition boundary between these two regions. Using available models for the prediction of the axial void fraction profile in subcooled flow boiling requires the accurate prediction of the location of the NVG point.

Most available models for predicting the void fraction profile in subcooled flow boiling, given below, were developed for high pressure flow. Their applicability in low pressure flow was found to be unsatisfactory [2–4]. In the present work, an accurate set of experimental data on subcooled flow boiling in annular channels is obtained and a new mechanistic model is developed. To put the present work into perspective, a summary of available models is given below.

† Author to whom correspondence should be addressed.

NOMENCLATURE

A	flow area
a_i	interfacial area concentration
Bo	boiling number, q/Gh_{fg}
C_p	liquid specific heat
C_v	condensation term, equation (13)
D_h	channel hydraulic diameter
D_s	mean Sauter bubble diameter
$(dP/dz)_f$	frictional pressure drop gradient
$(dP/dz)_t$	total pressure drop gradient
g	gravitational acceleration
G	mass flux
G_v	generation term, equation (18)
h_c	interfacial condensation coefficient
h_f	liquid enthalpy at saturation condition
h_{fg}	latent heat
h_g	vapour enthalpy at saturation
h_l	liquid enthalpy
h_{sh}	single phase heat transfer coefficient
Ja	Jakob number based on liquid subcooling, $\rho_l C_p(T_s-T_l)/\rho_g h_{fg}$
k	liquid thermal conductivity
Nu_c	interfacial Nusselt number, $h_c D_s/k$
P	pressure
P_h	heater perimeter
Pr	liquid Prandt number
q	wall heat flux
Re	flow Reynolds number, GD_h/μ
Re_b	bubble Reynolds number, $\rho_l u_b D_s/\mu$
T	temperature
u	velocity
u_b	bubble rise velocity
U_{gj}	drift vapour velocity
x	quality
z	axial location in z-direction.

Greek symbols

α	average void fraction
α_k	volumetric fraction of phase k
ε	pumping factor, equation (24)
μ	liquid dynamic viscosity
ρ	density
σ	surface tension
θ	subcooling temperature, T_s-T
$\Delta\rho$	$\rho_l-\rho_g$.

Subscripts

l	liquid
g	vapour
in	inlet conditions
s	saturation
th	thermal equilibrium
w	wall.

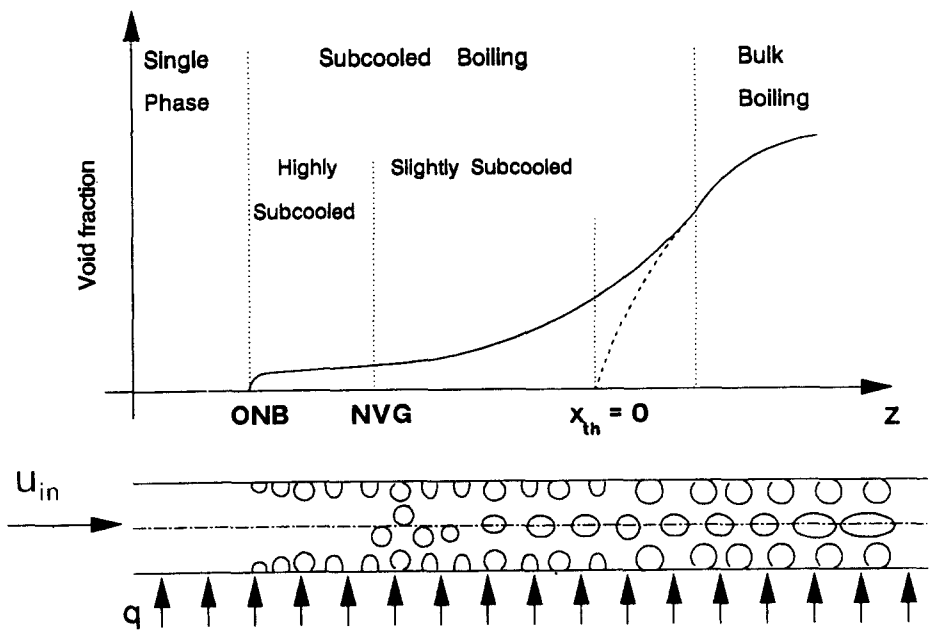

Fig. 1. Subcooled flow boiling regions.

2. REVIEW OF VOID FRACTION PROFILE MODELS

The available models can be divided into two categories; profile fit models and mechanistic models. The profile fit models are fully empirical, while the mechanistic models satisfy some conservation laws but use empirical relations for closure. All the available models, however, adapted the concept of two subcooled boiling regions, described above, and accordingly require knowledge of the location of the NVG point. Moreover, most of them assume that the void fraction in the highly subcooled region, upstream of the NVG point, is negligible. However, this may only be justified in high pressure flow.

2.1. *Profile fit models*

In this group of models, the void fraction profile is obtained by empirical correlations, e.g. the drift flux model of Zuber–Findlay [5], where the relationship between the void fraction and the true flow quality (vapour mass fraction) was obtained from:

$$\alpha = \frac{x}{\rho_g}\left[C_o\left(\frac{x}{\rho_g}+\frac{1-x}{\rho_l}\right)+\frac{U_{gj}}{G}\right]^{-1} \tag{1}$$

and the vapour drift velocity was calculated from:

$$U_{gj} = C_{zf}[\sigma g(\rho_l-\rho_g)/\rho_l^2]^{1/4} \tag{2}$$

where C_o and C_{zf} are empirical constants.

The thermodynamic quality profile along the flow passage was typically calculated using a simple energy balance. In subcooled flow boiling, the thermodynamic quality, calculated on the basis of thermodynamic equilibrium, is different from the true flow quality, which is the ratio of the vapour to the total mass flow rates. The true flow quality, in terms of the thermodynamic quality, was obtained using empirical relationships. Saha and Zuber [6], using the earlier work of Zuber *et al.* [7] and Kroeger and Zuber [8], assumed that the relationship between the true flow quality and the thermodynamic equilibrium quality could be predicted by:

$$x = \frac{x_{th}-x_d\exp(x_{th}/x_d-1)}{1-x_d\exp(x_{th}/x_d-1)} \tag{3}$$

where x_{th} is a thermodynamic quality, and x_d is a thermodynamic quality at the NVG point. The above expression satisfies the following boundary conditions: at the NVG point, where $x_{th} = x_d$, the net amount of vapour generated is very small, i.e. $x = 0$, and, at the transition from the subcooled boiling into bulk boiling ($x_{th} \gg x_d$), x approaches x_{th}. The above approach clearly requires a model, or a correlation, for the thermodynamic quality at the NVG point, x_d.

2.2. *Mechanistic models*

In these models, forms of the conservation equations are solved simultaneously along the heated channel to calculate the flow quality or the void fraction. The solution is typically complemented by an additional equation relating the void fraction to the quality, e.g. the drift flux model given by equation (1). In applying a mechanistic approach, various modelling issues arise; these are related to: (i) the division of the wall heat flux between vapour generation and the subcooled liquid; (ii) vapour condensation; (iii) vapour relative velocity, and (iv) bubble size or interfacial area concentration. A detailed review of these issues was given by Zeitoun [9]. A brief summary is outlined herein.

The heat removed from the heating surface is typically divided between the vapour and liquid phases. The first part is used to generate the vapour, while the second part is used to heat the subcooled liquid. In an early attempt, Griffith *et al.* [1] assumed that the total wall heat flux was used in evaporation while the liquid was heated only due to vapour condensation. Bowring [10] assumed that the liquid component consisted of a single phase forced convection component, predicted by known relations, and a pumping (agitation) component. The latter is caused by convection due to bubble nucleation and departure cycles. Bowring [10] defined a pumping factor, ε, which is the ratio between the pumping component and the vapour generation component, and used an empirical correlation for its estimation. Rouhani and Axelsson [11] neglected the single phase component based on the assumption that the heating surface was fully covered by bubbles downstream of the NVG point and considered the pumping component only. Ahmad [12] and Chatoorgoon [2, 13] combined both the liquid components into one. Ahmad [12] used the heat transfer coefficient correlated at the NVG point to predict the liquid component, while Chatoorgoon [2] used an empirical expression, based on the NVG location, for the fractional power that is responsible for vapour generation. Larsen and Tong [14] and Hancox and Nicoll [15] assumed the liquid component to be equal to the heat transfer rate at the edge of the bubble layer. Maroti [16] assumed the vapour component to equal the energy stored in the superheated liquid layer whose thickness was estimated from the conduction equation at the heating surface. Lahey [17] followed the division mechanism of Bowring [10] and Dix [18], but the single phase component was calculated from a linear function of the local subcooling. Sekoguchi *et al.* [19] estimated the vapour component from the difference between the fully developed turbulent radial temperature profile in single phase liquid flow and the measured radial temperature profile for flow boiling near a heating surface.

Another important issue in developing accurate mechanistic models for predicting void fraction distribution in subcooled flow boiling is the accurate estimation of the condensation rate. The condensation rate is a function of the local subcooling as well as the interfacial area concentration and interfacial heat transfer coefficient. Zeitoun *et al.* [20, 21] have addressed these issues in detail. Most available cor-

relations for interfacial condensation heat transfer are based on data obtained from single bubbles [21]. The interfacial area concentration, on the other hand, was either incorporated empirically in a condensation parameter [3, 11, 12] or calculated based on assuming an average bubble diameter to fit the data. A wide range of bubble diameters was used with little or no justification. While Chatoorgoon [2] assumed the bubble diameter to be 2.5 mm, Lai and Farouk [22] used 10 mm.

3. EXPERIMENTS

3.1. *Experimental facility*

A schematic of the test loop is presented in Fig. 2. The low pressure water boiling loop shown is described in detail by Zeitoun [9]. It consists of a holding tank, in which the distilled and degassed water temperature is controlled by an immersed electric heater and a cooling coil, a circulating pump, a preheater and the test section. The experiments were carried out in a vertical concentric annular test section. The outer tube was a 25.4 mm inner diameter plexiglass tube that allowed visual observation. The inner tube, which had an outside diameter of 12.7 mm, was made of three axial sections. The middle section of the inner tube was a 30.6 cm long, thin-walled stainless-steel tube (0.25 mm thickness), which was electrically heated. This heated section was preceded and followed by 34 cm long and 50 cm long, thick walled copper tubes, respectively. The entire inner tube was connected to a 55 kW DC power supply. Accordingly, heat was generated uniformly in the middle section where the subcooled boiling took place. The vapour formed in the boiling section was condensed in the adiabatic downstream section. The facility allowed accurate control of the inlet mass flux, wall heat flux and inlet subcooling.

The measurements carried out during the experiments included the inlet and exit fluid temperature, liquid subcooling distribution along the test section, wall heat flux, flow rate as well as the axial void fraction along the test section. High speed photography was also used to visualize the boiling phenomenon at various axial locations. A spring loaded sliding thermocouple, J type, was used to measure the temperature of the inner side of the heated tube. The measurements were conducted at 2 cm intervals along the heated section. Details of the thermocouple design and measurements were reported in Zeitoun [9]. Since the focus of the present paper is on the axial void fraction distribution, its measurement is discussed here in more detail.

A single beam gamma densitometer was used for void fraction measurements. It consisted of a 75 mCi ^{57}Co sealed line source and a cubic NaI (TI) scintillator. The gamma beam from the line source was collimated as a thin beam wide enough to cover the entire cross-section for measuring the area-averaged void fraction. The densitometer was operated in the count mode. The main signal processing system was described earlier by Zeitoun *et al.* [9, 20]. The gamma source and the scintillator were mounted on a vertically traversing table to obtain the axial area-averaged void fraction along the boiling section. For the present gamma densitometer design, the sensitivity to water content was about 20%. The sensitivity is defined by $S = (N_1 - N_0)/N_m$, where N_1 and N_0 are the count rates for empty and water filled test sections, respectively, and N_m is the mean value. The statistical error, defined by $\varepsilon = 1/S\sqrt{N}$, was reduced to less than 1–2% by counting for a long enough time. The densitometer was statically calibrated using an identical test section where the liquid phase was simulated by a Lucite plug, while the voids were generated by drilling holes into the plug. The static calibration tests showed that, for the range $0.02 < \alpha < 0.3$, the average uncertainty was within $\pm 4\%$ in the calibrated range. The maximum absolute error was estimated to be 0.015.

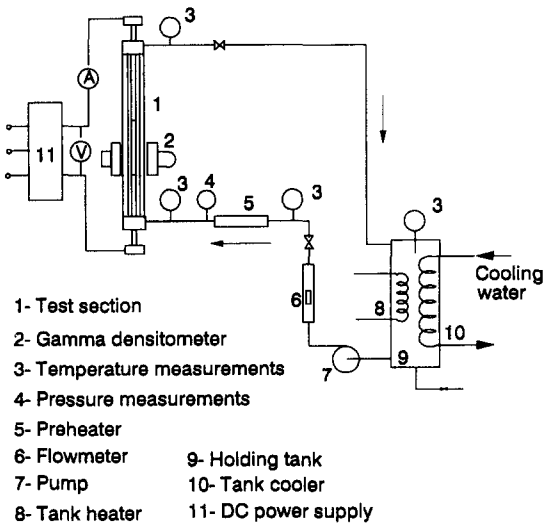

Fig. 2. Test loop.

3.2. *Experimental results*

A typical measured void fraction profile along the subcooled boiling region is shown in Fig. 3. As shown,

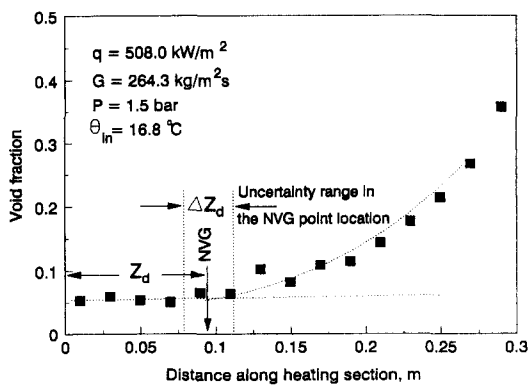

Fig. 3. Uncertainty in NVG point location.

the rate of increase of void fraction along the test section was very small in the upstream region resulting in an almost flat void profile with a void fraction typically in the range of 2–9%. The void fraction started to increase at a higher rate at a certain point defining the location of the NVG point. Detailed discussion of the NVG phenomenon in low pressure flow boiling was presented by Zeitoun and Shoukri [23]. The uncertainties in determining its location were also examined. Figure 3 demonstrates the method used for determining the NVG point. The present paper focuses on the axial void fraction profile. However, as discussed earlier, available models require prior knowledge of the NVG point location.

4. A MECHANISTIC VOID FRACTION PROFILE MODEL

4.1. *Model formulation*

The two-fluid model approach can, in principle, capture the non-equilibrium nature of subcooled flow boiling and as such is appropriate for modelling the void fraction profile. In this approach, the conservation equations of mass, momentum and energy are written for each phase k and the interfacial transport phenomenon is accounted for by interfacial terms. Following Ishii and Mishima [24], the one-dimensional two-fluid model can be simplified to:

- phase continuity equation

$$\frac{\partial}{\partial t}(\alpha_k \rho_k) + \frac{\partial}{\partial z}(\alpha_k \rho_k u_k) = \Gamma_k \tag{4}$$

- phase momentum equation

$$\frac{\partial}{\partial t}(\alpha_k \rho_k u_k) + \frac{\partial}{\partial z}(\alpha_k \rho_k u_k^2) + \alpha_k \frac{\partial P}{\partial z} - \alpha_k \rho = -F_{wk} - F_i - F_{ki} \tag{5}$$

- phase energy equation

$$\frac{\partial}{\partial t}\left(\alpha_k \rho_k \left(h_k + \frac{u_k^2}{2}\right)\right) + \frac{\partial}{\partial z}\left(\alpha_k \rho_k u_k \left(h_k + \frac{u_k}{2}\right)\right) - \alpha_k \frac{\partial P_k}{\partial t} - \alpha_k \rho_k u_k \boldsymbol{g} = q_i + q_{wk} + q_{ki}. \tag{6}$$

In the above equations, the subscript k refers to the phase k ($k = g$ for the vapour and $k = l$ for the liquid). The terms on the right-hand side of the above equations represent the interfacial transport terms. Γ_k is the rate of mass transfer into phase k per unit volume, F_{wk} is the wall friction force on phase k per unit volume, F_i is the interfacial force term, F_{ki} is a term representing the exchange of momentum associated with interfacial mass transfer, q_i is the interfacial heat exchange rate, q_{wk} is the wall heat transfer rate, and q_{ki} is a term representing the exchange of energy associated with interfacial mass transfer. The interfacial force term F_i is typically made of two terms, a drag force term and a virtual mass term.

For the present case of steady-state subcooled flow boiling through a channel, the above equations can be simplified by neglecting the transient terms and terms representing kinetic and potential energy. These terms are expected to be very small compared to the terms which include thermal energy. The above equations can be further simplified by summing up the phasic equations to obtain the mixture conservation equations. Following Zeitoun [9], the above equations can be reduced to the following governing equations:

- the mixture continuity equation

$$\frac{\mathrm{d}}{\mathrm{d}z}[\rho_l u_l (1-\alpha) + \rho_g u_g \alpha)] = 0 \tag{7}$$

- the vapour energy equation

$$\frac{\mathrm{d}}{\mathrm{d}z}[\rho_g h_g u_g \alpha] = G_v/A - C_v/A \tag{8}$$

- the mixture energy equation

$$\frac{\mathrm{d}}{\mathrm{d}z}[\rho_l C_p u_l T_l (1-\alpha) + \rho_g h_g u_g \alpha] = P_h q_l \tag{9}$$

- the mixture momentum equation

$$-\left(\frac{\mathrm{d}P}{\mathrm{d}z}\right)_t = \left(\frac{\mathrm{d}P}{\mathrm{d}z}\right)_f + \boldsymbol{g}[\rho_l (1-\alpha) + \rho_g \alpha] + \frac{\mathrm{d}}{\mathrm{d}z}[\rho_l u_l^2 (1-\alpha) + \rho_g u_g^2 \alpha]. \tag{10}$$

In the above equations, G_v and C_v are the rates of heat required for vapour generation and release due to vapour condensation per unit length along the boiling channel, respectively.

4.2. *Closure relationships*

The above four governing equations contain five unknowns, u_l, T_l, α, P and u_g, as well as three unknown terms G_v, C_v and the frictional pressure component. The vapour phase is assumed to be at saturation. To solve the above governing equations in the first four unknowns, a number of closure equations and assumptions are required. In the present analysis, the following relations and assumptions are used.

(1) Using the drift flux model of Zuber and Findlay [5], the vapour velocity was calculated from the following equation:

$$u_g = u_l + u_b \tag{11}$$

where the bubble relative velocity was calculated using the drift flux model of Zuber and Findlay [5],

$$u_b = \frac{1.53}{1-\alpha}[\sigma \mathbf{g}(\rho_l - \rho_g)/\rho_l^2]^{1/4}. \tag{12}$$

(2) The vapour condensation rate was modelled in terms of the interfacial condensation coefficient, interfacial area of condensing bubbles and the temperature difference across the liquid–vapour interface.

The rate of condensation per unit volume can accordingly be modelled by the following equation:

$$C_v/A = C_s a_i h_c (T_s - T_l) \tag{13}$$

where C_s is the fraction of the bubbles, or the interfacial area concentration, subjected to condensation, a_i is the interfacial area concentration, i.e. interfacial area per unit volume, and h_c is the interfacial heat transfer coefficient. The interfacial area concentration was calculated from the relation between the average bubble diameter and the void fraction; $a_i = 6\alpha/D_s$. The average bubble diameter was calculated from the correlation developed by Zeitoun and Shoukri [25] for the mean Sauter diameter of bubbles in low pressure subcooled flow boiling,

$$\frac{D_s}{\sqrt{\sigma/g\Delta\rho}} = \frac{0.0683(\rho_l/\rho_g)^{1.326}}{Re^{0.324}\left(Ja + \dfrac{149.2(\rho_l/\rho_g)^{1.326}}{Bo^{0.487}Re^{1.6}}\right)}. \tag{14}$$

(3) The interfacial condensation heat transfer coefficient required in equation (13) was calculated from the interfacial heat transfer correlation developed for subcooled water–steam bubbly flow by Zeitoun *et al.* [21],

$$Nu_c = 2.04 Re_b^{0.61} \alpha^{0.328} Ja^{-0.308}. \tag{15}$$

Alternatively, Akiyama [26] proposed the following equation for the interfacial condensation coefficient,

$$Nu_c = 0.37 Re_b^{0.6} Pr^{1/3}. \tag{16}$$

(4) The frictional pressure gradient component can be calculated from Chisholm's model [27] developed for evaporating flow. It should be noted that the results were insensitive to the choice of the frictional pressure drop model since the pressure drop encountered in the experiments, which were simulated, was very low.

(5) The remaining concern is the development of a model for dividing the applied wall heat flux between vapour generation and sensible heating of the liquid phase. Most of the available models were developed for high pressure flows and as such assume that the void fraction upstream of the NVG point is negligible. Recent void fraction measurements, including the present experimental work, indicate that the void fraction in this highly subcooled region is significant and in the range of 2–9%. In the present analysis, the entire subcooled flow boiling region is considered.

As mentioned earlier, the applied heat flux is divided into two components, a component that generates vapour at the heating surface and a second component that heats the subcooled liquid:

$$q = q_v + q_l. \tag{17}$$

The vapour generation term G_v appearing in equation (8) can be estimated from:

$$G_v = P_h q_v. \tag{18}$$

Following ONB, the condensation term cannot exceed the vapour generation term, although the two terms can be equal as the void fraction profile tends to be flat upstream of the NVG point. Accordingly, the following constraint should be satisfied:

$$G_v \geqslant C_v. \tag{19}$$

The liquid component, q_l, includes the heat transfer due to the single phase forced convection, which is proportional to the temperature difference between the heated surface and the liquid temperature, and the energy transfer due to the agitation of the thermal boundary layer caused by the bubble growth–collapse cycle. The last effect is referred to in the literature as the 'pumping' effect. The liquid component may be put in the form:

$$q_l = C_l h_{sp}(T_w - T_l) + q_p \tag{20}$$

where the parameter C_l accounts for the portion of the heating surface not covered by bubbles. The pumping component q_p includes effects caused by the bubble growth–collapse cycle. The single phase heat transfer coefficient h_{sp} can be calculated from the Dittus–Boetler correlation [28]. Accordingly, the vapour component of the applied heat flux is:

$$q_v = q - C_l h_{sp}(T_w - T_l) - q_p. \tag{21}$$

The ratio between the pumping and vapour components is called the pumping factor ε as defined by Bowring [10]. In Bowring's definition, the liquid volume pushed away from, and the vapour volume generated at, the heating surface were assumed equal. Assuming that the liquid is at saturation condition at the heating surface, Bowring [10] calculated the pumping factor as follows,

$$\varepsilon = \frac{\text{Vapour volume} \times \rho_l C_p (T_s - T_l)}{\text{Vapour volume} \times \rho_g h_{fg}}. \tag{22}$$

Following this procedure gives a high pumping factor which results in suppressing the vapour generation process. There are two aspects of discussion in Bowring's formulation. The energy transferred from the heating surface should be based on the volume of the thermal boundary layer pushed by the nucleating bubbles and the average temperature difference across the thermal boundary layer. Using this analysis, the pumping factor can be defined by:

$$\varepsilon = \frac{\dfrac{\Pi}{4} D_s^2 \delta_{th} \rho_l C_p \left(\dfrac{T_w + T_l}{2} - T_l\right)}{\dfrac{\Pi}{6} D_s^3 \rho_g h_{fg}} \tag{23}$$

or,

$$\varepsilon = \frac{3}{4} \frac{\rho_l C_p (T_w - T_l)}{\rho_g h_{fg}} \frac{\delta_{th}}{D_s} \tag{24}$$

where the thermal boundary layer thickness δ_{th} can be calculated from the following approximation:

$$\delta_{th} = \frac{k(T_w - T_l)}{q}. \quad (25)$$

The conservation equations, equations (7–10), can be solved simultaneously using the closure relationships described above and the appropriate boundary conditions. However, there are two remaining unknown parameters in equations (13) and (20)—C_s and C_l. The parameter C_l, which accounts for the portion of the heating surface not covered by bubbles, will be a function of the void fraction at the heating surface. To simplify the problem, this parameter will be assumed unity, $C_l = 1$. A sensitivity analysis has shown that the results are rather insensitive to the value of C_l within the range of conditions tested in this paper. The portion of interfacial area concentration in contact with the subcooled liquid, C_s, is expected to change along the heating section. However, no information is available on this change. For simplicity, the parameter C_s is assumed to be constant along the heating section. The effect of various methods of estimating C_s is examined in the following sections. This was done by either assuming a value for C_s or by estimating it at the NVG point by assuming that at this point there is a balance between the vapour generation and condensation rates, i.e. $G_v = C_v$.

In using the above closure equations, the wall temperature is required for calculating the single-phase component of the wall heat flux and the pumping factor. When comparing the model predictions with the present data, the measured wall temperature was used. However, in comparing the model's predictions with other data, for which the wall temperature was not used, the correlation of Shah [29] was used.

4.3. *Solution*

The Runge–Kutta method was used to integrate equations (7)–(10) simultaneously along the heating section. The boundary conditions at the heating section inlet, $z = 0$ were: $u_l = G/\rho_l$, $T_l = T_{in}$ and $\alpha = 0$. The last boundary condition, zero void fraction at the entry, caused mathematical overflow at $z = 0$. To overcome this difficulty, a very small void fraction was used at $z = 0$. Different values were checked, $\alpha = 0.00001$–0.001, and no effect was observed in the results.

5. RESULTS

5.1. *Effect of various closure assumptions on the solution*

A number of cases were examined to investigate the effect of various closure models on the solution. Four cases were examined. In the first case, the heat applied at the heating surface was divided between the liquid and vapour phase but the pumping component was neglected, i.e. $\varepsilon = 0$. The liquid component was calculated from the single phase forced convection. For the condensation term, 50% of the interfacial area concentration was assumed to be in contact with the subcooled liquid. Accordingly, identification of the NVG point was not needed. It was found that this case overpredicted the present data as shown in Fig. 4. In the second, third and fourth cases, the pumping component was calculated from the proposed model—equations (21) and (24). For the second and third cases, the portion of the interfacial area concentration, factor C_s, subject to condensation, was calculated at the NVG condition from the balance between the vapour generation and condensation rates. For the second case, the location of the NVG point was determined experimentally following the procedure described in Zeitoun and Shoukri [23] for the measured void fraction profiles as given in Fig. 3, while, for the third case, the location of the NVG point was calculated from the model proposed by Zeitoun and Shoukri [23]. In the fourth case, the NVG location was not required as the parameter C_s was assumed to be 50%, based on the average of the estimated values of this parameter in the second case.

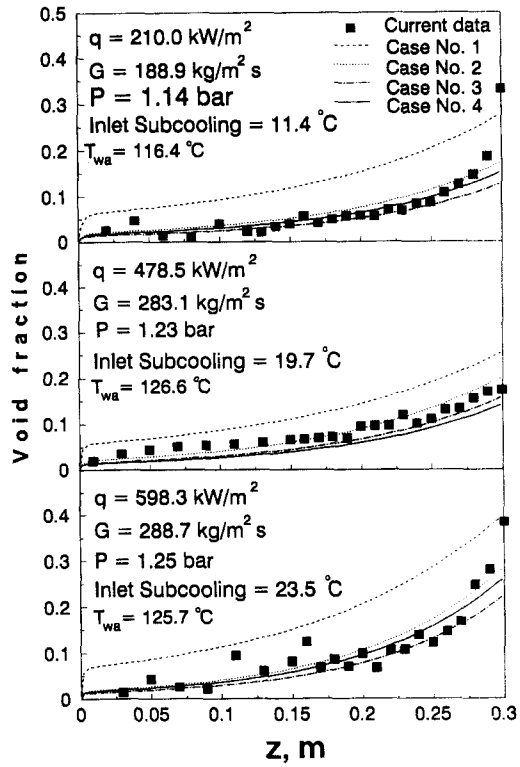

Fig. 4. Effect of various wall heat flux division models.

The void fraction profiles predicted using the assumptions associated with the above cases are compared with the values measured in the current investigation in Fig. 4. As shown in this figure, the void fraction starts from a very low value (0.001) and initially increases rapidly depending on the flux division model. The reason for the high void fraction gradient at the beginning is the absence of the vapour condensation function due to the very small value of the interfacial area present. As shown in the comparisons, the first case gives the highest void fraction

values. These high values resulted from neglecting the pumping component of the wall heat flux. Using the conditions at the NVG point located experimentally to calculate the parameter C_s, the second case gives good predictions of the void fraction profiles. This case is not practical because it needs prior experimental information on the NVG location which is unavailable during computational simulation. Using the conditions at the NVG point calculated from the NVG model developed by Zeitoun and Shoukri [23], to calculate the parameter C_s, the third case, gives reasonable profiles. However, the accuracy of this method depends on the accurate prediction of the NVG point. Note that the uncertainty margin of the available NVG models was found by Zeitoun and Shoukri [23] to be in the range of $\pm 30\%$ or higher. Therefore, using any NVG model is not expected to improve the prediction of the void fraction profile. Using a value of 50% for parameter C_s, the fourth case, gave an equally good agreement between the predicted and measured void fraction profiles. The interesting feature of this procedure is the independence from the NVG location, i.e. it was possible to obtain a reasonable void fraction profile without looking for the location of the NVG point. At this point, it can be concluded that an accurate void fraction profile can be obtained, provided that accurate information on the heat flux division and vapour condensation terms are available without prior knowledge of the location of the NVG point. This is particularly useful, given the uncertainty in defining the NVG point, particularly in low pressure flow boiling.

Further analysis was carried out to examine the effect of using various bubble condensation coefficients. The procedure described in the fourth case was followed but the interfacial condensation coefficient was calculated using the correlations of Zeitoun *et al.* [21] and Akiyama [26]. In this case, the vapour generation rate was calculated using the proposed heat flux division model. Half of the interfacial area concentration was assumed to be in contact with subcooled liquid, i.e. $C_s = 0.50$.

Comparisons between the void fraction profiles predicted from the model using both interfacial condensation coefficients are superimposed on the present data in Fig. 5. As shown in this figure, the Zeitoun *et al.* [21] bubble condensation model gives lower condensation rates, and accordingly higher void fractions,

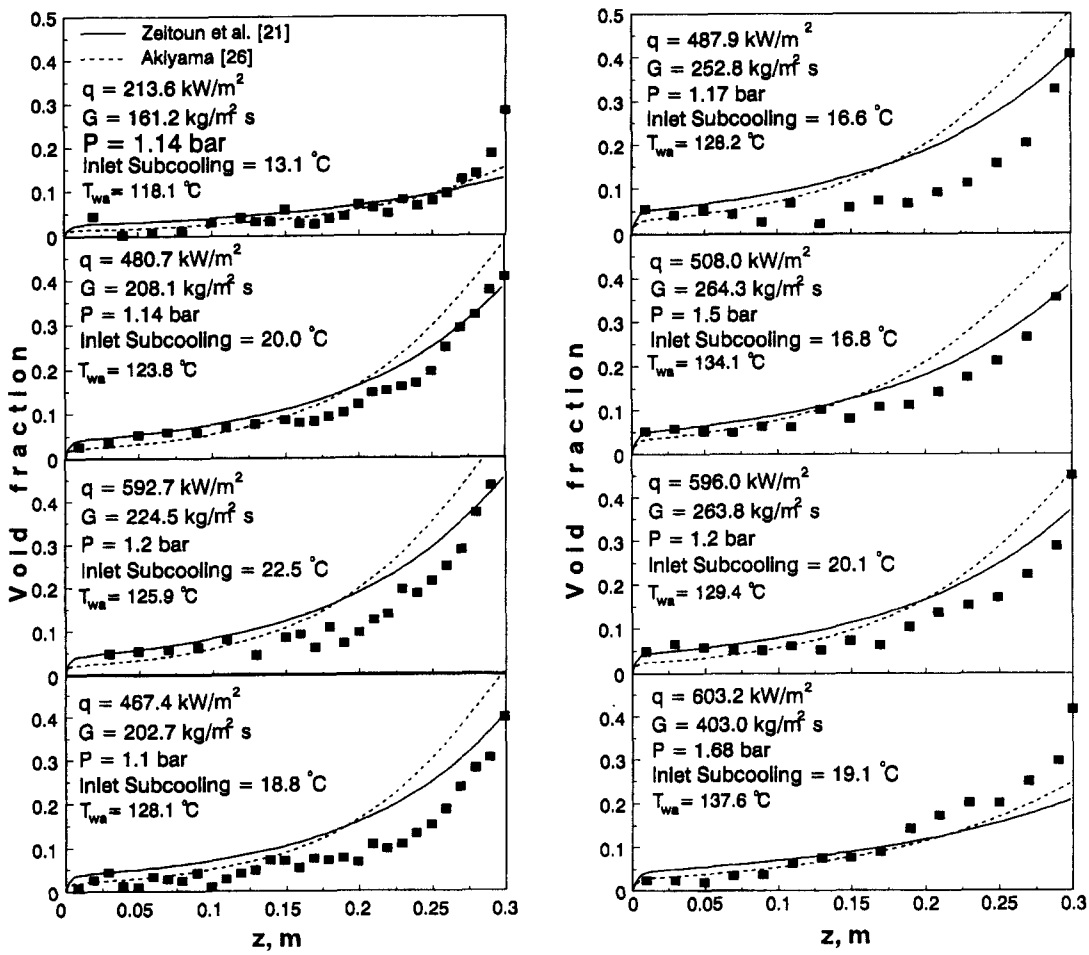

Fig. 5. Effect of using different interfacial condensation coefficients.

than that of Akiyama [26] in the low void fraction region. However, this trend is reversed in the high void fraction region. This is caused by the dependence of the bubble condensation model of Zeitoun *et al.* on the void fraction. In general, using the interfacial heat transfer correlation developed by Zeitoun *et al.* [21] for subcooled liquid–vapour bubbly flow gave better results than using Akiyama's model. Near the end of the heating section where bubble coalescence is a major factor, the present model gave lower predictions. This is expected since the closure models used only considered the bubbly flow regime.

5.2. *Comparison with available data*

Comparisons between the predicted void fraction profiles using the present model and available data from the literature are shown in Figs. 6–9. It should be mentioned that these data were obtained using the gamma attenuation technique in different channel geometries and for water–steam flow at low pressure (1–2 bar). The data of Donevski and Shoukri [30] were measured in the present test section. The data of Dimmick and Selander [31] were measured for subcooled flow boiling inside a tube of 12.29 mm inside diameter. The data of Rogers *et al.* [32] and Bibeau and Salcudean [33] were measured in annular channels of hydraulic diameters of 8.9 mm and 9.1 mm, respectively. As shown, the present model predicted most of these data reasonably well. However, it significantly

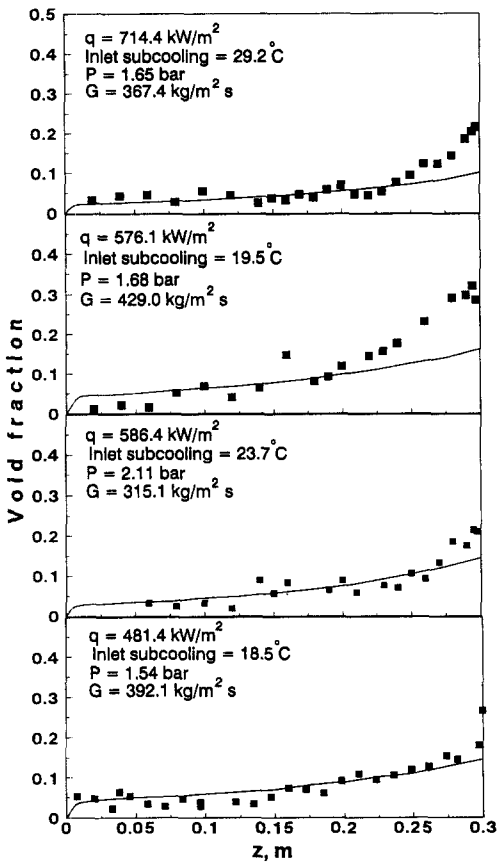

Fig. 6. Comparison between the predicted void fraction and the data of Donevski and Shoukri [30].

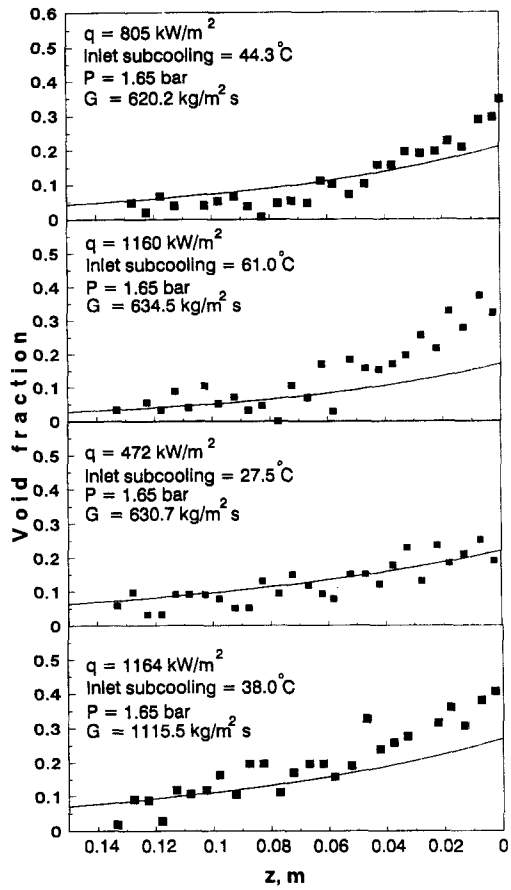

Fig. 7. Comparison between the predicted void fraction and the data of Dimmick and Selander [31].

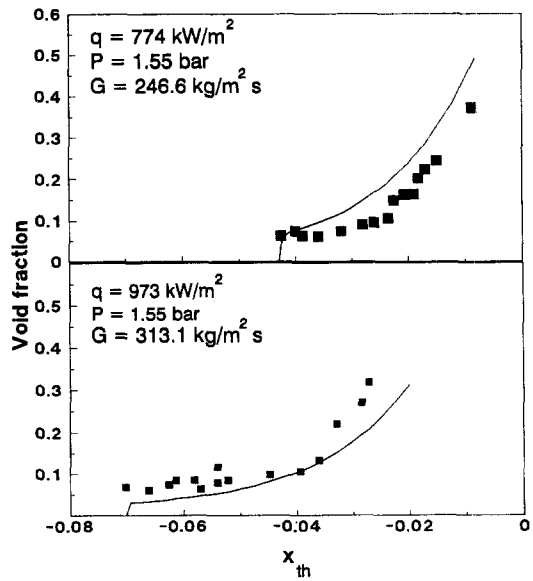

Fig. 8. Comparison between the predicted void fraction and the data of Rogers *et al.* [32].

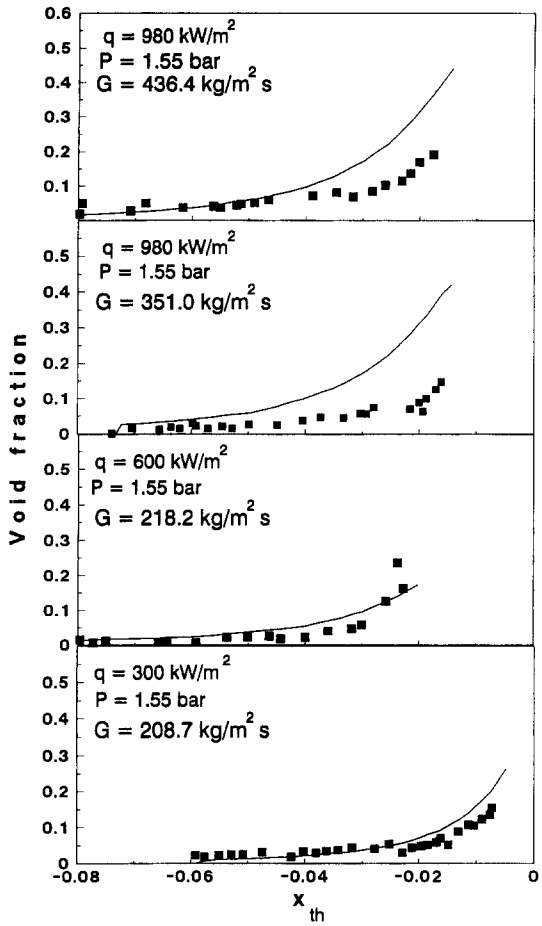

Fig. 9. Comparison between the predicted void fraction and the data of Bibeau and Salcudean [33].

overpredicted the first two cases in the data of Bibeau and Salcudean [33]. The measured void fractions in these two cases are particularly low when compared with the data measured by Rogers *et al.* [32] which were obtained under similar test conditions.

6. CONCLUDING REMARKS

Experimental data on axial void fraction profiles in subcooled flow boiling region along an annular vertical channel were obtained for various levels of mass flux, heat flux and inlet subcooling using a single-beam gamma densitometer. A mechanistic model for the void fraction profile was introduced and various closure relationships were investigated. A wall heat flux division model was proposed by modifying Bowring's pumping factor [10]. The applicability of the correlation developed by Zeitoun *et al.* [21] for the interfacial heat transfer coefficient in subcooled water–steam bubbly flow was examined. The proposed mechanistic model was capable of predicting the axial void fraction profiles along both regions of the subcooled flow boiling. The location of the NVG point is not required in the model.

Acknowledgements—This work was funded by a joint grant from Atomic Energy of Canada Ltd. (AECL) and the Natural Science and Engineering Research Council (NSERC) of Canada. The support and technical input of Dr. V. Chatoorgoon of AECL was greatly appreciated.

REFERENCES

1. Griffith, P., Clark, J. A. and Rohsenow, W. M., Void volumes in subcooled boiling. ASME paper 58-HT-19, *National Heat Transfer Conference*, Chicago, 1958.
2. Chatoorgoon, V., A generation–condensation void fraction transport model for low pressure. In *Two-Phase Flow and Energy Exchange System*, HTD Vol. 220, eds. M. S. Sohel and T. J. Rabes. ASME, New York, 1992.
3. Chatoorgoon, V., Dimmick, G. R., Carver, M. B. and Shoukri, M., Application of generation and condensation models to predict subcooled boiling void at low pressure. *Nuclear Technology*, 1992, **98**, 366–378.
4. Evangelisti, R. and Lupoli, P., The void fraction in an annular channel at atomspheric pressure. *International Journal of Heat & Mass Transfer*, 1969, **12**, 699–711.
5. Zuber, N. and Findlay, J., Average volumetric concentration in two-phase flow system. *Journal of Heat Transfer*, 1965, **87**, 453–462.
6. Saha, P. and Zuber, N., Point of Net Vapour Generation and Vapour Void Fraction in Subcooled Boiling, *Proceedings of Fifth International Heat Transfer Conference*, Vol. 4, pp. 175–179. Tokyo, 1974.
7. Zuber, N., Staub, F. W. and Bijwaard, G., Vapour void fraction in subcooled boiling systems, *Proceedings of the Third International Heat Transfer Conference*, Vol. 5, pp. 24–38. Chicago, 1966.
8. Kroeger, P. G. and Zuber, N., An analysis of the effects of various parameters on the average void fraction in subcooled boiling. *International Journal of Heat & Mass Transfer*, 1968, **11**, 211–233.
9. Zeitoun, O., Subcooled flow boiling and condensation. Ph.D. thesis, McMaster University, Hamilton, ON, 1994.
10. Bowring, R. W., Physical model based on bubble detachment and calculation of steam voidage in the subcooled region of a heated channel. Report HPR-10, Institute for Atomenergi, Halden, Norway, 1962.
11. Rouhani, S. Z. and Axelsson, E., Calculation of void volume fraction in the subcooled and quality boiling region. *International Journal of Heat & Mass Transfer*, 1970, **13**, 383–393.
12. Ahmad, S. Y., Axial distribution of bulk temperature and void fraction in a heated channel with inlet subcooling. *Journal of Heat Transfer*, 1970, **92**, 595–609.
13. Chatoorgoon, V., Dimmick, G. R. and Carver, M. B., Modelling of low pressure subcooled boiling instability experiments. In *Instability in Two-Phase Flow Systems*, HTD-Vol. 260, ed. J. H. Kim. ASME, New York, 1993, pp. 41–51.
14. Larsden, P. S. and Tong, L. S., Void fraction in subcooled boiling. *Journal of Heat Transfer*, 1969, **91**, 471–476.
15. Hancox, W. T. and Nicoll, W. B., A general technique for the prediction of void distributions in non-steady two-phase forced convection. *International Journal of Heat & Mass Transfer*, 1971, **14**, 1377–1394.
16. Maroti, L., Axial distribution of void fraction in subcooled boiling. *Nuclear Technology*, 1977, **34**, 8–17.
17. Lahey, R. T., A mechanistic subcooled boiling model, *Sixth International Heat Transfer Conference*, Toronto, ON, pp. 293–297, 1978.
18. Dix, G. E., Vapour void fraction for forced convection

with subcooled boiling at low flow rates. General Electric report no. NEDO-10491, 1970.
19. Sekoguchi, K., Tanaka, O., Esaki, S. and Imasaka, T., Prediction of void fraction in subcooled and low quality boiling regions. *Bulletin of the JSME*, 1980, **23,** 1475–1482.
20. Zeitoun, O., Shoukri, M. and Chatoorgoon, V., Measurement of interfacial area concentration of subcooled liquid–vapour flow. *Nuclear Engineering and Design*, 1994, **152,** 243–255.
21. Zeitoun, O., Shoukri, M. and Chatoorgoon, V., Interfacial heat transfer between steam bubbles and subcooled water in vertical upward flow. *Journal of Heat Transfer*, 1995, **117,** 402–407.
22. Lai, J. C. and Farouk, B., Numerical simulation of subcooled and low quality forced convection boiling flows. *ANS Proceedings, National Heat Transfer Conference*, Vol. 6, pp. 12–20, 1992.
23. Zeitoun, O. and Shoukri, M., On the net vapour generation phenomenon in low pressure and mass flux subcooled flow boiling, *Proceedings of the Engineering Foundation Conference on Convective Flow Boiling*, Alberta, Canada, 1995.
24. Ishii, M. and Mishima, K., Two-fluid model and hydrodynamic constitutive relations. *Nuclear Engineering and Design*, 1984, **82,** 107–126.
25. Zeitoun, O. and Shoukri, M., Bubble behaviour and mean diameter in subcooled flow boiling. *Journal of Heat Transfer*, 1996, **118,** 110–116.
26. Akiyama, M., Bubble collapse in subcooled boiling. *Bulletin of the JSME*, 1973, **16,** 570–575.
27. Chisholm, D., Pressure gradients due to friction during the flow of evaporating two-phase mixtures in smooth tubes and channels. *International Journal of Heat & Mass Transfer*, 1973, **16,** 347–358.
28. Incropera, F. P. and Dewitt, D. P., *Introduction to Heat Transfer*. Wiley, 1985, p. 360.
29. Shah, M. M., General prediction of heat transfer during subcooled boiling in annuli. *Heat Transfer in Engineering*, 1983, **4,** 24–31.
30. Donevski, B. and Shoukri, M., Experimental study of subcooled flow boiling and condensation an annular channel. Thermofluids Report no. ME/89/TF/R1, Department of Mechanical Engineering, McMaster University, Hamilton, ON, 1989.
31. Dimmick, G. R. and Selander, W. N., A dynamic model for predicting subcooled void : experimental results and model development. EUROTHERM Seminar #16, Pisa, Italy, 1990.
32. Rogers, J. T., Salcudean, M., Abdullah, Z., McLeod, D. and Poirier, D., The onset of significant void in upflow boiling of water at low pressure and low velocities. *International Journal of Heat & Mass Transfer*, 1987, **30**(11), 2247–2260.
33. Bibeau, E. L. and Salcudean, M., The effect of flow direction on void growth at low velocities and low pressure. *International Communications in Heat & Mass Transfer*, 1990, **17,** 19–25.